AIP | Applied Physics Letters

The instability of silicene on Ag(111)

A. Acun, B. Poelsema, H. J. W. Zandvliet, and R. van Gastel

Citation: Applied Physics Letters **103**, 263119 (2013); doi: 10.1063/1.4860964
View online: http://dx.doi.org/10.1063/1.4860964
View Table of Contents: http://scitation.aip.org/content/aip/journal/apl/103/26?ver=pdfcov
Published by the AIP Publishing

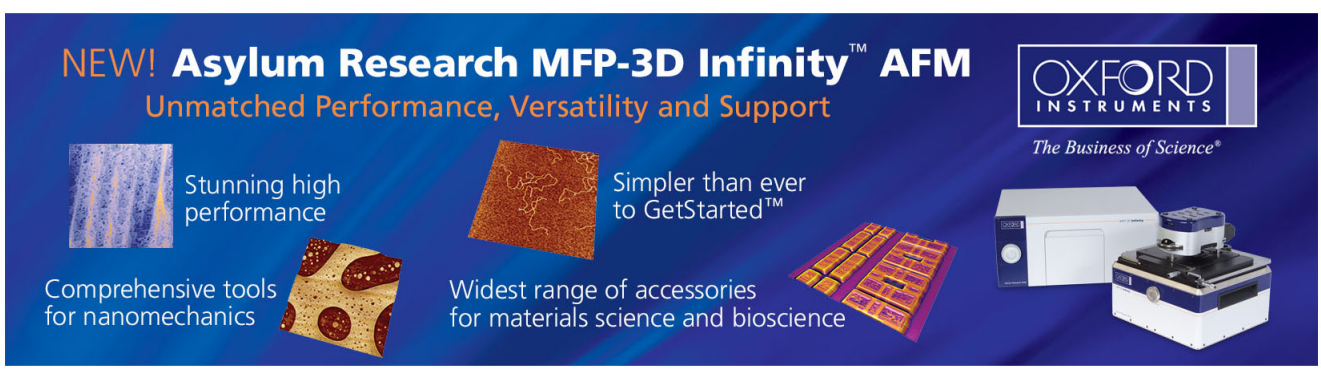

The instability of silicene on Ag(111)

A. Acun, B. Poelsema, H. J. W. Zandvliet, and R. van Gastel
Physics of Interfaces and Nanomaterials, MESA+ Institute for Nanotechnology, University of Twente, P.O. Box 217, 7500 AE Enschede, The Netherlands

(Received 28 October 2013; accepted 15 December 2013; published online 31 December 2013)

We have used low energy electron microscopy to directly visualize the formation and stability of silicene layers on a Ag(111) substrate. Theoretical calculations call into question the stability of this graphene-like analog of silicon. We find that silicene layers are intrinsically unstable against the formation of an "sp^3-like" hybridized, bulk-like silicon structure. The irreversible formation of this bulk-like structure is triggered by thermal Si adatoms that are created by the silicene layer itself. To add injury to insult, this same instability prevents the formation of a fully closed silicene layer or a thicker bilayer, rendering the future large-scale fabrication of silicene layers on Ag substrates unlikely. © *2013 AIP Publishing LLC*. [http://dx.doi.org/10.1063/1.4860964]

Silicene is the "sp^2-like" hybridized variant of silicon that forms part of a broader class of two-dimensional materials that exhibit exotic physical properties. For example, the integer quantum Hall effect as well as the Klein paradox were observed in graphene, silicene's carbon sister material.[1–5] Since silicon atoms share the same valence electron configuration as carbon, the emergence of graphene as a potential replacement for silicon in integrated circuits has recently triggered numerous theoretical, experimental, and computational studies of silicene.[6–11] Initial experiments made by Aufray *et al.*[12] and Le Lay,[13] using various techniques, led to the discovery and an accurate description of the structural properties of silicene. Furthermore, recent theoretical and experimental works suggest the existence of multilayers of silicene. The properties of multilayer silicene are rather exotic. Dirac fermions and superconductivity have been theoretically predicted,[14,15] and observations of the former have already appeared in literature.[16] The primary goal of most studies was to establish similarities with graphene, specifically whether or not electrons in silicene behave as massless Dirac fermions that obey the relativistic Dirac equation, which yields a linear dispersion relation for the electrons with relativistic Fermi velocities.[17] From a practical perspective, the very high mobility of electrons in these two-dimensional materials could be utilized in next-generation devices and replace silicon in integrated circuits.[9]

Experimentally, the first challenge that has been addressed is to verify that the growth of silicene layers is possible. So far, hints for the existence of silicene have been provided by scanning tunneling microscopy (STM),[9,11] atomic force microscopy (AFM),[18] low energy electron diffraction (LEED),[10,19] and angle-resolved photoemission spectroscopy (ARPES).[13,20] Silicon is typically deposited on a Ag(111) substrate. The silicon honeycomb lattice is almost perfectly commensurate with Ag(111), which also has a low tendency to form a Ag-Si alloy, thus making it an ideal substrate for the growth of silicene. A few remarks are in place here. First, density functional theory calculations by Wang *et al.*[17] suggest that the observed linear dispersion curve at the K point of the first Brillouin zone[13] originates from the underlying Ag(111) substrate. Second, it should be noted here that silicon honeycomb lattices can also occur for silicides.[21] Two other substrates that have also been used to grow silicene are ZrB_2[20] and Ir.[22] The most common overlayer structure of silicene on Ag(111) is (4×4).[23] Other phases that have been observed and reproduced are $(\sqrt{13} \times \sqrt{13})R13.9°$,[9] $(\sqrt{3} \times \sqrt{3})$,[10] $(\sqrt{7} \times \sqrt{7})$,[11] and $(2\sqrt{3} \times 2\sqrt{3})R30°$.[11] Furthermore, a distinct temperature and coverage dependence of the overlayer structure was reported.[10,19] While STM and AFM achieve atomic resolution, both techniques lack the ability to perform real-time imaging of changes in surface topography through surface diffusion, sublimation, growth, phase transitions, adsorption, and chemical reactions. LEED experiments exclusively yield reciprocal space information and would not suffice for collecting the desired data. Here, we have used a combination of low energy electron microscopy[24] (LEEM) and micro-LEED (μLEED) to directly image the growth and decay of Si on Ag(111) on a length scale of several microns and verify the structure and energetic stability of silicene layers.

An Elmitec LEEM III microscope[24] operated at a base pressure of 1×10^{-10} mbar was used for the experiments. The sample, a Ag(111) single crystal (Surface Preparation Laboratory) was cleaned by sputtering with argon and annealing at 700 K. The deposition of silicon was performed by heating a silicon wafer to approximately 1350 K. The deposition rate was derived from the 1022 s required to obtain a maximum fractional coverage of 0.96 (see Fig. 1 and corresponding discussion). Assuming a single layer of silicene, we arrive at a rate of 1.65×10^{-2} Si-atoms per nm^2 per s. In view of the potential bilayer character of the silicene that is mentioned elsewhere,[10] we emphasize that although a double layer of silicene would double this rate, it will not affect the basic conclusions of this paper. All LEEM images were recorded in bright-field mode with an electron energy of 18.3 eV at various fields of view (FOV) and sample temperatures. In all images, silicene and bulk-like silicon structures appear dark, whereas the Ag(111) substrate appears bright. μLEED was performed by inserting an aperture of 1.4 μm diameter into the incident electron beam to acquire localized diffraction patterns. To include all spots in a diffraction pattern during one specific experiment and unambiguously

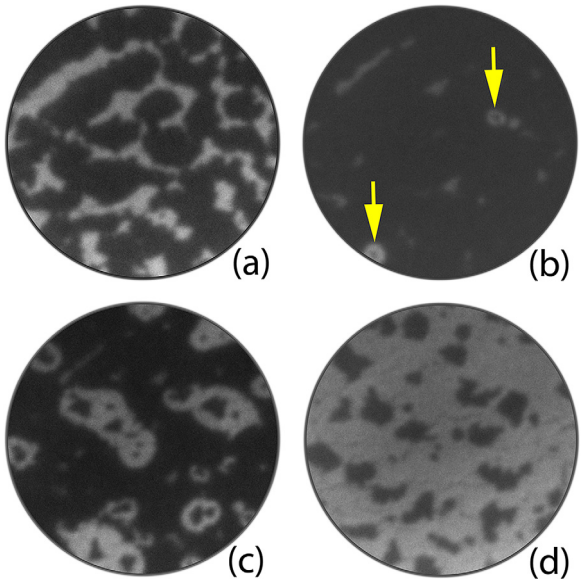

FIG. 1. Evolution of silicene morphology during growth on Ag(111). (a) Measured LEEM image of the initial growth and expansion of Si domains on Ag(111). (b) The Si covered fraction of the substrate increases, but then starts a steady decline after reaching a maximum coverage of 0.96 at 1022 s. (c) and (d) The decrease in fractional coverage continues 1142 s and 1394 s into the experiment before settling at a final value of 0.13.

establish the superstructure symmetry, a series of μLEED measurements were performed with an electron energy varying from 3.0 eV to 42.1 eV in steps of 0.1 eV, whereafter the patterns were accumulated into a single image. In the text, this type of experiment is referred to as cumulative LEED.

The deposition of silicon atoms on Ag(111) at 542 K is marked by an increase in the amount of diffuse scattering from the substrate prior to the nucleation of any islands.[25–27] This indicates the formation of a lattice gas of mobile silicon monomers (or multimers). When the lattice gas density becomes sufficiently supersaturated, silicon islands nucleate and grow. Figure 1(a) shows a 1.2 μm LEEM image of the silicon domains (dark) that have formed on Ag(111) (bright) after 766 s of deposition. As the Si coverage is further increased, one would intuitively expect the nucleation of a second layer on top of the first one. However, just before reaching the point where the substrate is covered with a full monolayer of silicon, the projected silicon coverage decreases dramatically, as is shown in Figs. 1(b)–1(d). Furthermore, in Fig. 1(b), when the maximum area percentage is reached, two small silicon features indicated by arrows located in the center of a circular area of bare Ag(111) are discernible at locations that are different from those where the original silicon domains nucleated in Fig. 1(a). These features slowly grow in size at the expense of the initial layer in Figs. 1(b)–1(d). The bare substrate area around the features rapidly expands. After reaching a maximum projected coverage of 0.96, the fraction of the substrate that is still covered by Si structures at the end of the experiment (Fig. 1(d)) is reduced to 0.13. This considerable change in projected area hints at a three-dimensional nature of the observed features. A simple division of 0.96×0.13 gives 7.4, which corresponds to the height of the converted layer, where we assumed that the in-plane density of both the initial islands and the features that form later is identical.

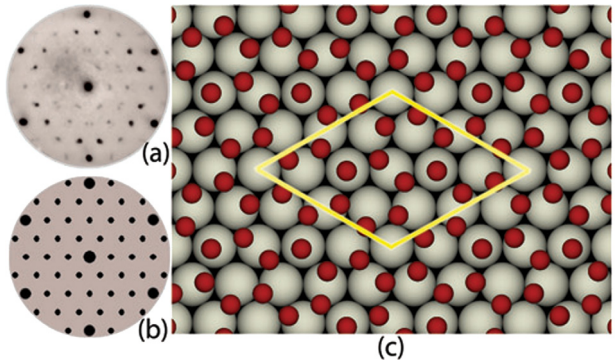

FIG. 2. Experimental and calculated μLEED patterns of silicene islands. (a) Cumulative μLEED pattern of the initial silicene islands. The symmetry of the superstructure phase corresponds to a $(2\sqrt{3} \times 2\sqrt{3})$R30°, which identifies it as "sp^2-like" hybridized or *silicene*. The spot splitting is caused by the interference of electron beams that are independently reflected from the silver substrate and the silicon layer, respectively. (b) The calculated LEED pattern of the same structure. (c) The unit cell of the real space structure that corresponds to the LEED pattern shown in panel (a).

The structure of the initial islands was characterized through cumulative μLEED measurements at 553 K. The result is depicted in Fig. 2(a). The superstructure symmetry of the initial islands is $(2\sqrt{3} \times 2\sqrt{3})$R30°. We have used *LEEDPat30*[28] to simulate the data, as shown in Fig. 2(b). The experimental and computational data fit very well. A careful comparison of both images reveals that the experimental data exhibits spot splitting in some spots, whereas the simulated pattern does not. Figure 2(c) depicts the real space structure that corresponds to the LEED patterns. The relatively large unit cell of the initial layer periodically exposes a significant portion of the silver atoms of the substrate to incident electrons. Reflected electron beams from the silicon layer and the exposed silver substrate will interfere as a function of primary energy according to Bragg's law. We tentatively deem this interference responsible for the spot splitting, since it leads to spot splitting at (near-) destructive interference conditions. Because the pattern that we recorded is a cumulative μLEED pattern where the electron energy was ramped, the spot splitting is always observed in the final pattern. The measured superstructure was already assigned to silicene,[11,19] or "sp^2-like" hybridized silicon. The configuration in Fig. 2(c) does not show a clear preference for the occupation of high symmetry sites on Ag(111), hinting to a weak coupling between silicene and Ag(111).

Knowing that the layer that initially forms is silicene, the next question that needs to be addressed is what the structure and conversion mechanism is of the features that form later in the experiment. Again, μLEED was used to record diffraction patterns on top of one of the converted features. The pattern that was recorded at an energy of 31.0 eV is shown in Fig. 3(a). Because the size of the features is below the size of the smallest illumination aperture in our LEEM, a significant Ag(111) background is present in the pattern. The symmetry of the superstructure can however still be extracted from the pattern. The features exhibit a $(\frac{1}{2}\sqrt{21} \times \frac{1}{2}\sqrt{21})$R10.9° structure, which was confirmed through the simulation shown in Fig. 3(b). An almost similar overlayer structure, $(4/\sqrt{3} \times 4/\sqrt{3})$, was found by Arafune *et al.*,[10] but assigned to bilayers of silicene. The ratio of the

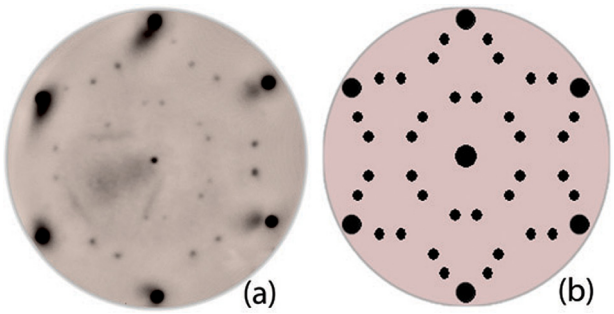

FIG. 3. Experimental and calculated μLEED pattern of bulk-like "sp^3-like" hybridized silicon features on Ag(111). (a) μLEED pattern recorded on a "sp^3-like" hybridized silicon feature at room temperature at an electron energy of 31.0 eV. The symmetry of the superstructure is $(\frac{1}{2}\sqrt{21} \times \frac{1}{2}\sqrt{21})$R10.9° and corresponds to bulk-like silicon. (b) A simulation of the "sp^3-like" hybridized, where in this case the spot splitting is due to different rotational domains.

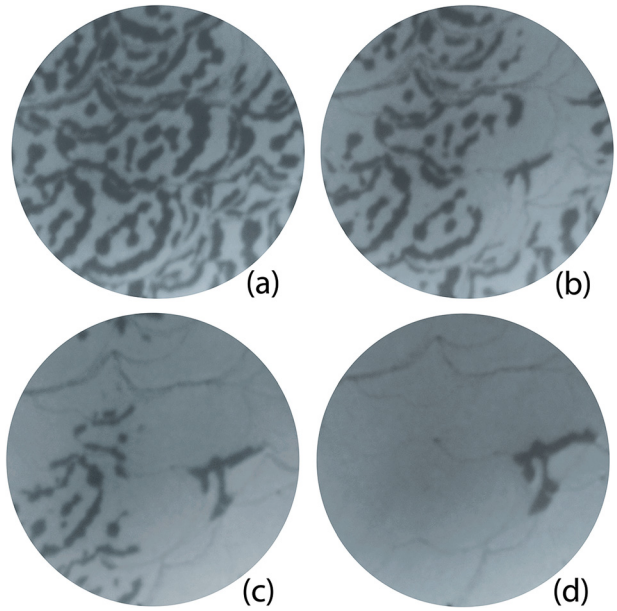

FIG. 4. Thermally induced phase transition of silicene from an "sp^2-like" to "sp^3-like" hybridized state. (a) The initial configuration of silicene islands (dark) on the Ag(111) substrate (bright) at 548 K. (b) During a temperature increase to 629 K, the islands reduce in size due to an increase in silicon adatom spreading pressure. (c) Upon reaching 629 K, a silicene-denuded zone appears around an "sp^3-like" hybridized domain. (d) The "sp^3-like" hybridized domains expand at the expense of the silicene until eventually all silicene islands are consumed.

area of the unit cell of the converted layer to that of the substrate is 1.75 when one unit cell contains three atoms. On the other hand, the ratio of a_{Si}^2 to a_{Ag}^2 is 1.763, where a_{Si} (5.431 Å) and a_{Ag} (4.090 Å) are the bulk lattice parameters of silicon and silver. This observation hints at a "sp^3-like" hybridized, 3D nature of these silicon features. However, it should be pointed out that the areal density of a silicene layer on Ag(111)[11,13] is only moderately larger than that of a Si "bilayer" at Si(111) surfaces. The "sp^3-like" hybridized state of silicon is induced by the nucleation of second-layer islands on top of the silicene when the first silicene monolayer is close to completion. The energetic stability of the bulk-like silicon is so much greater[8] that it consumes all thermal silicon adatoms that are emitted from the silicene layers, leading to the formation of circular, silicene-denuded zones around the nucleation sites of the sp^3 features, and ultimately, the complete disappearance of all silicene domains.

The transition from "sp^2-like" hybridized silicene to "sp^3-like" hybridized bulk-like silicon is induced by an increased spreading pressure of silicon adatoms on top of the silicene layers. In the experiment of Fig. 1, the increased spreading pressure was simply the result of the deposition of additional material from the Si evaporator. In a separate experiment, we grew silicene until a moderate projected coverage close to half a monolayer was reached, as shown in the 2.4 μm field of view LEEM image in Fig. 4(a). At this stage, the deposition of silicon atoms on the substrate was abruptly stopped. The temperature was gradually increased from 548 K to 629 K and was kept stable there. Silicene islands disappear in time at 629 K in a manner that is similar to that of Figs. 1(b)–1(d) and at a temperature that is comparable to what was observed by Feng *et al.*[11] In addition to the disappearance of the silicene domains, we again observe the growth of another feature at the heart of the silicene-denuded zones, as illustrated in Figs. 4(b)–4(d). μLEED measurements were performed on this object and yielded a $(\frac{1}{2}\sqrt{21} \times \frac{1}{2}\sqrt{21})$R10.9° structure, identical to that of Fig. 3(a), and corresponding to "sp^3-like" hybridized silicon. The structural transition from an "sp^2-like" to "sp^3-like" configuration indicates that "sp^2-like" hybridized silicene is an energetically unfavorable configuration of silicon that is easily perturbed by the presence of silicon adatoms on top of the silicene. This statement holds irrespective of whether those adatoms are the result of the growth process itself, i.e., the near-completion of a silicene layer, or whether it is the result of an increased spreading pressure due to an increased temperature. This scenario is distinctly different for carbon, where the sp^3 hybridized state (diamond) is less stable than sp^2 hybridized carbon (graphite/graphene)[29] at room temperature and atmospheric pressure. Another significant difference between graphene and silicene is found in the temperatures where a phase transition such as that in Fig. 4 occurs. The temperature induced phase transition for silicene on Ag(111) occurred at approximately 600 K, while that of graphene occurs at markably higher temperatures.[30]

In summary, the growth of silicene on Ag(111) was studied in-situ with LEEM and μLEED. While silicene islands nucleate and grow during the initial stages of the deposition of silicon, a phase transition occurs from "sp^2-like" to "sp^3-like" hybridized silicon before the surface can be fully covered by silicene. The same phase transition can be induced by increasing the substrate temperature, thereby raising the equilibrium density of silicon adatoms on top of the silicene layers. The occurrence of this change in hybridization makes the controlled fabrication of single layer, closed silicene sheets problematic, at least when using Ag substrates, which are commonly considered ideal due to their minute misfit. Either the deposition process itself or the adatoms originating from the silicene domains themselves induce the irreversible structural transition and cause the silicene to self-destruct. Our results further demonstrate that, whereas theoretical considerations predict that the pure form of silicene is energetically stable, its actual, practical

stability can only be appropriately judged by considering the environment that the silicene is in. This implies that coupling of the silicene layer to the substrate, and its interaction with adatoms may crucially influence the delicate stability of the silicene epitaxial layer, much more so than for graphene, and need to be taken into account. Other, more complex multilayer silicene structures, which were not observed in the present study, are anticipated to be even more susceptible to the observed instability.

[1]H. W. Kroto, J. R. Heath, S. C. O'Brien, R. F. Curl, and R. E. Smalley, Nature **318**, 162–163 (1985).
[2]K. S. Novoselov, A. K. Geim, S. V. Morozov, D. Jiang, Y. Zhang, S. V. Dubonos, I. V. Grigorieva, and R. E. Smalley, Science **306**, 666–669 (2004).
[3]C. L. Kane and E. J. Mele, Phys. Rev. Lett. **95**, 146802 (2005).
[4]Y. Zhang, Y.-W. Tan, H. L. Stormer, and P. Kim, Nature **438**, 201–204 (2005).
[5]M. I. Katsnelson, K. S. Novoselov, and A. K. Geim, Nat. Phys. **2**, 620–625 (2006).
[6]S. Cahangirov, M. Topsakal, E. Aktürk, H. Şahin, and S. Ciraci, Phys. Rev. Lett. **102**, 236804 (2009).
[7]E. F. Sheka, Int. J. Quantum Chem. **113**, 612–618 (2013).
[8]K. Takeda and K. Shiraishi, Phys. Rev. B **50**, 14916–14922 (1994).
[9]C.-L. Lin, R. Arafune, K. Kawahara, N. Tsukahara, E. Minamitani, Y. Kim, N. Takagi, and M. Kawai, Appl. Phys. Express **5**, 045802 (2012).
[10]R. Arafune, C.-L. Lin, K. Kawahara, N. Tsukahara, E. Minamitani, Y. Kim, N. Takagi, and M. Kawai, Surf. Sci. **608**, 297–300 (2013).
[11]B. Feng, Z. Ding, S. Meng, Y. Yao, X. He, P. Cheng, L. Chen, and K. Wu, Nano Lett. **12**, 3507–3511 (2012).
[12]B. Aufray, A. Kara, S. Vizzini, H. Oughaddou, S. Léandri, B. Ealet, and G. Le Lay, Appl. Phys. Lett. **96**, 183102 (2010).
[13]P. Vogt, P. De Padova, C. Quaresima, J. Avila, E. Frantzeskakis, M. C. Asensio, A. Resta, B. Ealet, and G. Le Lay, Phys. Rev. Lett. **108**, 155501 (2012).
[14]Z.-X. Guo and A. Oshiyama, e-print arXiv:1309.6412 [cond-mat.mes-hall].
[15]F. Liu, C.-C. Liu, K. Wu, F. Yang, and Y. Yao, Phys. Rev. Lett. **111**, 066804 (2013).
[16]P. de Padova, P. Vogt, A. Resta, J. Avila, I. Razado-Colambo, C. Quaresima, C. Ottaviani, B. Olivieri, T. Bruhn, T. Hirahara, T. Shirai, S. Hasegawa, M. C. Asensio, and G. Le Lay, Appl. Phys. Lett. **102**, 163106 (2013).
[17]Y.-P. Wang and H.-P. Cheng, Phys. Rev. B **87**, 245430 (2013).
[18]Z. Majzik, M. Rachid Tchalala, M. Svec, P. Hapala, H. Enriquez, A. Kara, A. J. Mayne, G. Dujardin, P. Jelínek, and H. Oughaddou, J. Phys. Condens. Matter **25**, 225301 (2013).
[19]H. Jangotchian, Y. Colignon, N. Hamzaoui, B. Ealet, J.-Y. Hoarau, B. Aufray, and J. P. Bibérian, J. Phys. Condens. Matter **24**, 172001 (2012).
[20]A. Fleurence, R. Friedlein, T. Ozaki, H. Kawai, Y. Wang, and Y. Yamada-Takamura, Phys. Rev. Lett. **108**, 245501 (2012).
[21]P. Wetzel, S. Saintenoy, C. Pirri, D. Bolmont, and G. Gewinner, Phys. Rev. B **50**, 10886 (1994).
[22]L. Meng, Y. Wang, L. Zhang, S. Du, R. Wu, L. Li, Y. Zhang, G. Li, H. Zhou, W. A. Hofer, and H. J. Gao, Nano Lett. **13**, 685–690 (2013).
[23]H. Enriquez, S. Vizzini, A. Kara, B. Lalmi, and H. Oughaddou, J. Phys. Condens. Matter **24**, 314211 (2012).
[24]E. Bauer, Rep. Prog. Phys. **57**, 895–906 (1994).
[25]J. de la Figuera, N. C. Bartelt, and K. F. McCarty, Surf. Sci. **600**, 4062 (2006).
[26]D. Schwarz, R. van Gastel, H. J. W. Zandvliet, and B. Poelsema, Phys. Rev. Lett. **109**, 016101 (2012).
[27]D. Schwarz, R. van Gastel, H. J. W. Zandvliet, and B. Poelsema, Phys. Rev. B **85**, 235419 (2012).
[28]K. Hermann and M. A. van Hove, LEEDPat30 (v3.0) software package (2013), http://www.fhi-berlin.mpg.de/KHsoftware/LEEDpat/.
[29]R. Webster and P. G. Read, *Gems: Their Sources, Descriptions and Identification* (Butterworth-Heinemann, Saint-Louis, Missouri, USA, 1994).
[30]P. Sutter, J. Flege, and E. Sutter, Nature Mater. **7**, 406–411 (2008).